RESEARCH ARTICLE

New Metallophthalocyanines Posture Pyridine Pendants Via 1,3,4-Oxadiazole Bridge: Synthesis, Optical and Electrical Studies

Chemical Sciences Journal, Vol. 2013: CSJ-105

New Metallophthalocyanines Posture Pyridine Pendants Via 1,3,4-Oxadiazole Bridge: Synthesis, Optical and Electrical Studies

Pradeep K Musturappa[1], Venugopala KR Reddy[2]*, Harish MN Kotresh[3], Chidananda Basappa[1], Madhu B Jayanna[4], Mruthyunjayachari C Devendrachari[1], Fasiulla[5]

[1]Department of Industrial Chemistry, Sahyadri Science College (Autonomous), Kuvempu University, Shivamogga 577203, Karnataka, India.

[2]Department of Chemistry, Vijayanagara Sri Krishnadevaraya University, Bellary 583104, Karnataka, India.

[3]PG Department of Chemistry, JSS College of Arts, Commerce and Science, Ooty Road, Mysore 25, Karnataka, India.

[4]Department of Physics, Government Science College, Chitradurga 577501, Karnataka, India.

[5]Department of Chemistry, Manipal Institute of Technology, Manipal, Karnataka, India.

***Correspondence:** venurashmi30@gmail.com

Accepted: Apr 17, 2013; Published: May 6, 2013

Abstract

The new symmetrically tetra substituted metallophthalocyanines (MPc) [MPc1-3, M = Co(II), Ni(II) and Cu(II)] bearing pyridyl moieties on peripheral positions have been synthesized via 1,3,4-oxadiazole bridge. The newly prepared compounds have been characterized by elemental analysis, FTIR, Solid State ^{13}C NMR, Solid State UV–Vis, Thermogravimetric Analysis (TGA) and XRD analysis, the complexes are in good consistency with the experimental results. All the newly synthesized compounds exhibited good optical property showing the red shift of Q-band position and TGA results show admirable thermal stability (>400 °C). The MPc2 and 3 show high dielectric constant (ε'), 9800 and 11150 respectively, at 50 Hz. The ensuing MPc1-3 show low dielectric loss (tanδ) in the frequency range of 50 Hz to 5 MHz at room temperature. The shoulder nature is observed in the variation of tanδ with frequency for MPc2 and MPc3, which is understood on the basis of resonance between hopping frequencies of charge carriers and applied frequency. The variation of AC conductivity with frequency was explained by electron hopping model and values are in the range of 4.0×10^{-5}–1.6×10^{-4} (S/m) at 5 MHz measured at 20 °C.

Keywords: Metallophthalocyanine; pyridine; dielectric studies; 1,3,4-oxadiazole.

1. Introduction

Phthalocyanines (Pcs) have attracted considerable interest due to their unique optical and electrical properties. Recently, much attention has been focused on substituted Pcs because their properties can be extensively modified by varying the metal and peripheral substituents. Metallophthalocyanines (MPc) are organic materials with semiconducting properties. Therefore, the study of these compounds is very essential to understand the behaviour of their electronic and physical properties under various conditions such as changes in frequency, temperature, pressure, ambient gases, etc. [1, 2]. The electronic properties of MPc have received increasing attention because of their importance as prototype semiconductors and their uses in technological applications such as solar cells, gas sensors [3] and to generate various types of switching devices [4]. It also finds applications in nonlinear optical (NLO) devices [5], liquid crystals, Langmuir–Blodgett films, electrochromic devices [6, 7], photodynamic therapy of cancer (PDT) [8] and catalysis [9]. The high dielectric constant materials have possible application in electromechanical fields such as high performance sensors, actuators as well as bypass capacitors in microelectronics and energy-storage devices [10, 11]. The growing use of Pcs as advanced materials during the last decade has encouraged research on the synthesis of new derivatized materials.

The aromatic heterocyclic moieties like oxadiazole, pyridine, quinoline, thiadiazoles and triazoles, have been suggested as good electron transport and hole blocking materials for electroluminescent devices [12-14]. And on the whole 1,3,4-oxadiazole derivatives are important organic semiconducting materials and widely used in photo-electronic devices [15]. Our recent contributions describing a series of Pcs with aryl and alkyl-[1,3,4]-oxadiazole subunits which exhibited admirable optical, thermal and electrical properties [16, 17]. To the best of our knowledge, very few reports are available on tetra and octa substituted pyridine on Pc

periphery via ether (O) and thiaether (S) linkage and suit for PDT, electrochemical and photochemical studies [18-20].

Therefore, in this contribution, we inserted the pyrido-[1,3,4]-oxadiazole moieties onto electron-rich MPc periphery (Scheme 1) (MPc1-3, M = Co(II), Ni(II) and Cu(II)). The resulting complexes were characterized by elemental analysis, FTIR, Solid state ^{13}C NMR, Solid state UV–Vis, TGA, XRD analysis and further subjected to electrical studies. Measurements of AC conductivity of semiconductors have been extensively used to understand the conduction mechanisms in these materials [21]. In the present work, the frequency dependence of AC conductivity, dielectric constant and dielectric loss studies have been performed for MPc1-3 in bulk form. The measurements have been carried out in the frequency range of 50Hz to 5 MHz at room temperature.

2. Methods

2.1. Materials

1,2,4-Benzene tricarboxylic anhydride and Isoniazide were purchased from Sigma Aldrich and Polyphosphoric acid (PPA) was purchased from Himedia Chemicals Ltd. India. All the other chemicals were procured from SD-Fine Chemicals, and used as received. Tetracarboxy metal phthalocyanines (TCMPc) [M = Co, Ni and Cu] were prepared according to the described procedure [22].

2.2. Instrumentation

Elemental analysis was obtained from a Carlo-Erba 1106 instrument. FTIR spectra were recorded on a FT-IR 8400s Shimadzu spectrometer in KBr pellets. Solid state electronic absorption spectra were recorded on a UV-Vis NIR spectrometer, model USD 4000. Solid-state ^{13}C-NMR spectra were recorded on a Bruker DSX-300 solid-state NMR spectrometer with a magnetic field of 7.04 T and carbon frequency of 75.47 MHz (internal standard was glycine). Perkin-Elmer Thermal analyzer was used for TGA. Powdered XRD measurements were carried out on a Bruker D8 Advance X-ray diffractometer. The dielectric and AC conductivity measurements were carried out using impedance analyzer model HIOKI 3352-50 HiTESTER Version 2.3.

2.3. Synthesis

General procedure for Tetra-pyrido-[1,3,4]-oxadiazole substituted MPc complexes (MPc1–3) [Scheme 1]

Tetra-pyrido-[1,3,4]-oxadiazole substituted MPc1-3 were synthesized by adopting the procedure earlier reported by us [16, 17]. In brief, TCMPc (0.001 mol) and Isoniazide (pyridine-4-carbohydrazide) (0.006 mol) were stirred in preheated 100 g polyphosphoric acid (PPA) containing 10g P_2O_5 and the reaction mixture was maintained at 150 °C for 20h. The product obtained was repeatedly treated with 0.1 N sodium hydroxide followed by water to remove unreacted TCMPc and unreacted isoniazide was removed by washing several times with hot water and acetone to get pure tetra-pyrido-[1,3,4]-oxadiazole substituted MPc complexes (MPc1–3).

Tetra-{pyrido-[1,3,4]-oxadiazole}-cobalt phthalocyanine (MPc1)

Yield: 92%. Calcd: C (62.57), H (2.45), N (24.32), O (5.56). Found: C (62.19), H (2.09), N (24.04), O (5.38). IR [(KBr) υ_{max}/cm^{-1}]: 2934 (Ar–CH), 1609 (C=N), 1518 (C=C), 1141 (-C-O), 1096, 925, 831, 765 (Pc skeleton vibration). UV-Vis (solid state)λ_{max}/nm 432, 579, 795.

Tetra-{pyrido-[1,3,4]-oxadiazole}-nickel phthalocyanine (MPc2)

Yield: 90%. Calcd: C (62.57), H (2.45), N (24.32), O (5.56). Found: C (62.12), H (2.11), N (24.09), O (5.17). IR [(KBr) υ_{max}/cm^{-1}]: 2926 (Ar–CH), 1610 (C=N), 1531 (C=C), 1141 (-C-O), 1091, 926, 831, 766 (Pc skeleton vibration). ^{13}C-NMR (solid state) δ ppm 164, 150, 144, 132, 122. UV-Vis (solid state) λ_{max}/nm 433, 587, 835.

Tetra-{pyrido-[1,3,4]-oxadiazole}-copper phthalocyanine (MPc3)

Yield: 89%. Calcd: C (62.57), H (2.45), N (24.32), O (5.56). Found: C (62.08), H (2.01), N (24.04), O (5.19). IR [(KBr) υ_{max}/cm^{-1}]: 2932 (Ar–CH), 1610 (C=N), 1541 (C=C), 1140 (-C-O), 1093, 913, 832, 764 (Pc skeleton vibration). UV-Vis (solid state)λ_{max}/nm 435, 577, 814.

2.4. Electrical measurements

Devices were fabricated in a sandwich configuration Ag/MPc/Ag with powdered MPc(1-3), samples were compressed into pellets and conducting silver paint (ELTECKS preparation No. 1228-C) was coated on both flat

surfaces of the pellets and the electrical contacts to the samples were made using the same silver paint to the electrodes. The electrical contacts were checked to verify the ohmic connection. The dielectric and AC conductivity measurements were carried out using impedance analyzer model HIOKI 3352-50 HiTESTER Version 2.3. The measurements were carried out at room temperature in between the 50Hz–5MHz. The capacitance value (C), and AC conductance (G) were directly obtained from the instrument. The dielectric constant (ε') and AC conductivity (σ_{ac}) values are calculated using the relations $\varepsilon' = C_p d/\varepsilon_o A$ and $\sigma_{ac} = Gd/A$ respectively, where 'd' is the thickness of the sample and 'A' is the cross-section area and ε_o is the permittivity of the free space.

3. Results and Discussion

Melt condensation of tetracarboxy transition metal phthalocyanines with pyridine-4-carbohydrazide resulted in the formation of 2,9,16,23-tetra-pyrido-[1,3,4]-oxadiazole-substituted metal phthalocyanines (MPc1-3) (M = Co, Ni and Cu). The condensation was realized in the presence of PPA at 150-160 °C. All the new Pc complexes were characterized by elemental analysis, FT-IR, solid-state UV-Vis, solid-state ^{13}C-NMR spectroscopy, TGA and XRD studies.

Scheme 1: Synthesis of tetra-pyrido-[1,3,4]-oxadiazole substituted MPcs1-3 (M= Co, Ni and Cu) complexes.

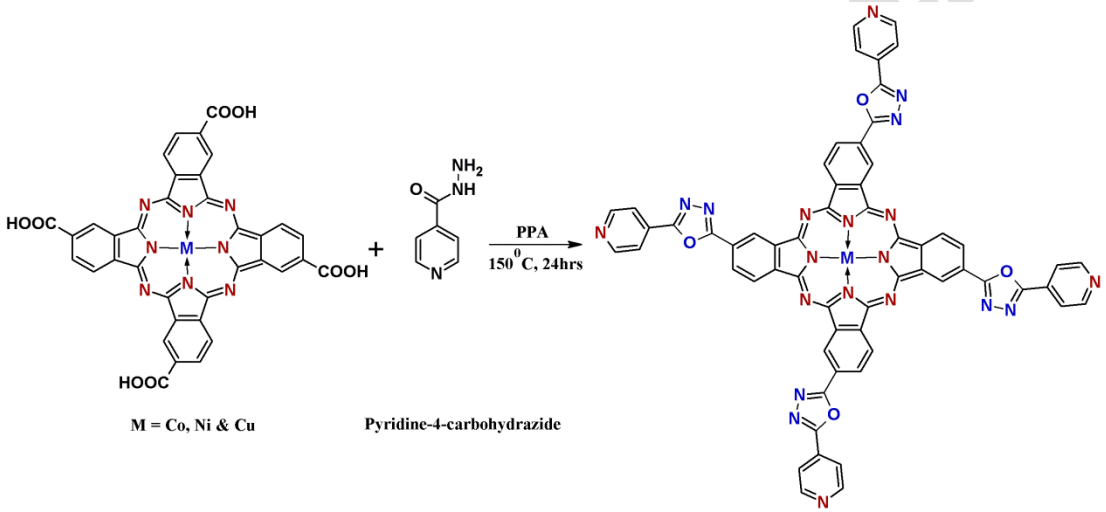

FT-IR spectra of complexes MPc1-3 exhibited a series of absorptions at 764–766, 831–832, 913–926 and 1091–1096 cm^{-1} which can be attributed to the Pc skeleton. Peaks at 1609–1610 and 1514–1541 cm^{-1} for MPc1-3 are assigned to aromatic –C=N– and –C=C– in plane skeletal vibrations of the Pc core. Peaks at 2926–2933 cm^{-1} and 1091–1096 cm^{-1} are associated with aromatic –C–H stretching and aromatic –C–H bending vibrations respectively. Comparison of FT-IR spectra of basic TCMPc and ensuing MPc1-3 reveals some marked differences; the characteristic intense absorption due to –C=O (–COOH) of TCMPc (M = Co, Ni and Cu) at ~1700 cm^{-1} disappear in the IR spectra of MPc1-3 indicating the involvement of carboxyl group in condensation followed by cyclization with pyridine-4-carbohydrazide. The characteristic stretching vibrations due to -C=N- and -C-O- for oxadiazole and -C=N- for pyridine rings are found to be coupled with skeletal vibrational peaks of –C=N–, –C=C– and of the Pc core.

Solid-state ^{13}C-NMR spectra of complex MPc2 are present in Figure 1. The MPc2 exhibit the expected broad signal at 122-132 ppm for aromatic carbons assigned as 'd' and 'e' in Figure 1. The peak at 144 ppm for oxadiazole moiety attached to aromatic carbons assigned as 'c' and carbons attached to nitrogen shows signal at 150 ppm named as 'b' respectively. Peaks at 164 ppm were assigned to oxadiazole carbon named as 'a' in Figure 1. Unfortunately, NMR spectroscopy is uniformative in case of cobalt and copper metal centres, because the paramagnetic character prevents the resolution of the signals [23].

Electronic absorption spectra are fruitful to establish the structure of phthalocyanines. Solid-state electronic absorption spectra of compounds MPc1-3 are presented in Figure 2. Pc have two allowed electronic transitions leading to two characteristic absorption bands in the UV–Vis spectrum: the Soret band (B bands), which appears at near-UV region and Q-band, both bands correspond to π–π* transitions. The location of the Soret bands (B bands) is quite similar for all MPc1-3 in range 432-435 nm and the characteristic Q-band appeared in the range 577-587 nm with marginal splitting along with an additional band of considerable

intensity in near-IR region at ≈ 800 nm. The presence of heteroaromatic ring systems (oxygen and nitrogen) in the MPc1-3 periphery lead to immense extension of π-conjugation inducing red shift and splitting of the Q-band, which may be attributed to a_{2u}-e_g and b_{2u}-e_g transitions [24] indicating effective electronic communiqué between the two different ring systems with Pc core. Further, the peak broadening is due to aggregation of Pc molecules owing to extended conjugation [25].

Figure 1: Solid-state C^{13} spectra of NiPc2.

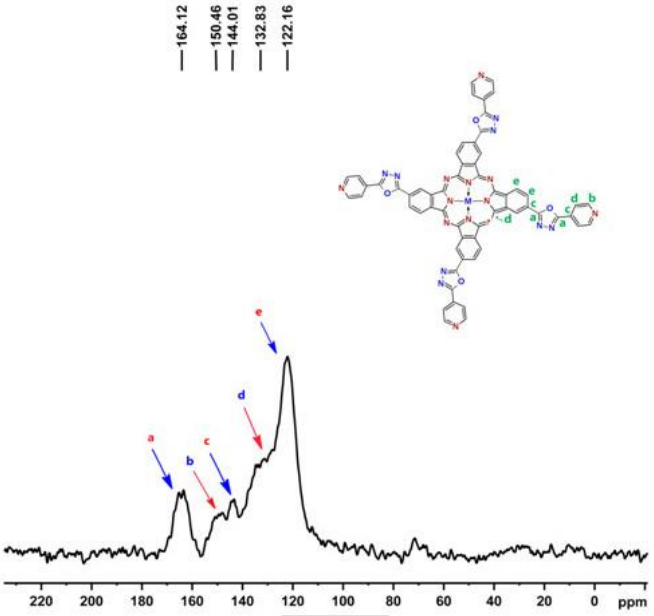

Figure 2: Solid-state electronic absorption spectra of MPc1-3 complexes.

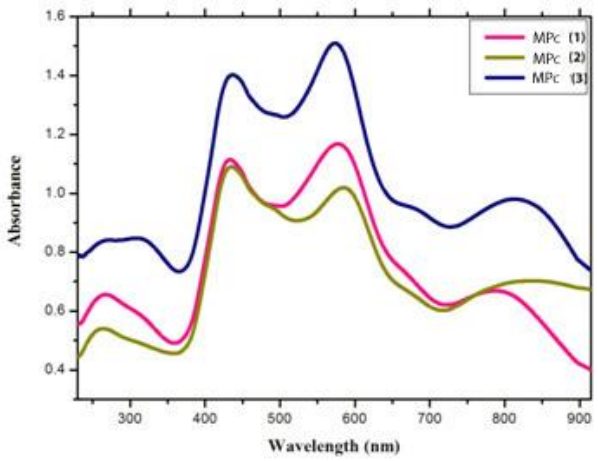

Optical band gaps of complexes MPc1-3 were determined by the absorption lower edge of the absorption spectrum of each compound in the solid state and the data are summarized in Table 1. Interactions of MPc molecules are of Van Der Waals type and the presence of heteroaromatic ring systems in the MPc periphery results in rearrangements of molecule and alter the energy band gap between valence and conduction bands.

Table 1: Optical band gap data of MPc1-3.

Samples	Peaks λ_{max} (nm)	Band gap (eV)
MPc1	432	2.87
	579	2.14
	795	1.55
MPc2	433	2.86
	587	2.11
	835	1.48
MPc3	435	2.85
	577	2.14
	814	1.52

Thermo gravimetric investigation of MPc1-3 complexes presented in Figure 3 indicates that the complexes undergo decomposition in two steps. The first step of the degradation in the temperature region around 110 °C may be accounted for the loss of moisture. The second step decomposition of MPc-1 observed in the temperature range of 412-520 °C and for MPc2 and 3 shows second step decomposition almost in the same temperature range of 460-570 °C. Among these, MPc-1 show early decomposition and MPc2 and 3 are almost same stability. The thermal analysis yields the stability of MPc1-3 complexes, all shows stability > 400 °C.

Figure 3: TGA graphs of MPc1-3 complexes.

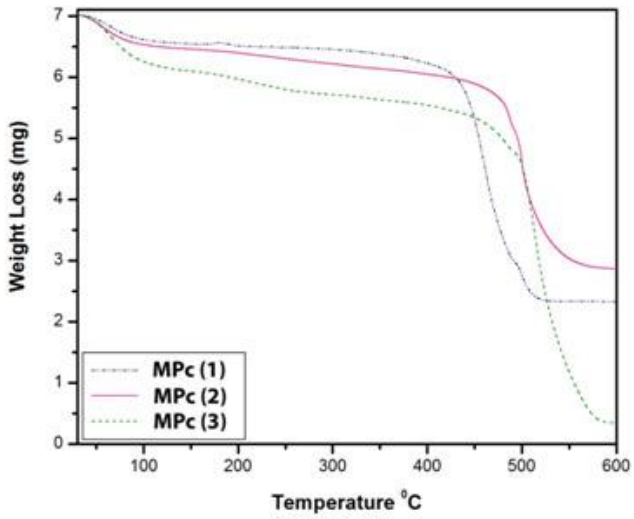

Kinetic and thermodynamic parameters were computed using Broido's method [26]. Plots of -Ln(ln(-1/Y)) versus 1/T (Figure 4) (where Y is the fraction of the compound undecomposed) were developed for the decomposition segment. From the plots, the activation energy (Ea) and frequency factor (ln A) were evaluated. The enthalpy (ΔH), entropy (ΔS) and free energy (ΔG) have been computed using standard equations and are summarized in Table 2.

The powdered XRD patterns of MPc1-3 are presented in Figure 5. The diffraction pattern exhibited characteristic broad peaks. The heteroaromatic pyrido-[1,3,4]-oxadiazole moieties in the Pc periphery result in extended conjugation and the greater π-electron region influences the stacking of the Pcs in parallel molecules and the ensuing compounds were amorphous in nature.

The AC electrical studies has been measured for bulk MPc in the form of compressed pellet Ag/MPc/Ag (M= Co, Ni and Cu) in the frequency range of 50 Hz to 5 MHz utilizing an oscillating voltage with amplitude 1V peak-to-peak. Results have been reported for pellets of MPc1-3 maintained under vacuum. Figure 6 shows variation of dielectric constant (ε′) with frequency for the complexes MPc1-3 at room temperature. Initially, ε′ decreases with increase in frequency and finally at higher frequencies reaching a constant value for all the complexes MPc1-3. The observed large values of ε′ at lower frequencies are attributed to the charge carriers present in the material (MPc), which migrate upon the application of the field. The decrease in ε′ may be due to the decrease in space charge carries or interfacial polarization in the Pc material [27]. At low frequencies,

the dipoles align themselves along the field and contribute fully to the total polarization. At higher frequencies, variation in the field is too rapid for the dipoles to align themselves. So, ε' variation is small, becomes nearly frequency independent and approaches a constant value as can be seen clearly in Figure 4. This can be attributed to rapid polarization process [28]. The high dielectric constant revealed MPc2 and 3 (9800 and 11500 at 50 Hz) finds the place in the field of sensors, actuators as well as bypass capacitors in microelectronics and energy-storage devices.

Figure 4: Plots of -Ln(ln(-1/y)) vs 1/T x 10^{-3} for the decomposition of MPc1-3 complexes.

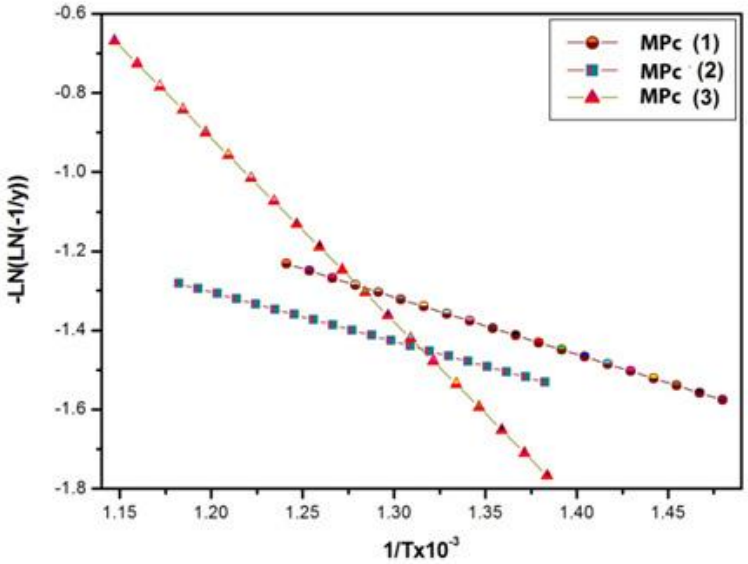

Table 2: Kinetic and thermodynamic parameters of MPc1-3.

Samples	Decomposition Range (°C)	Ea (kJ/mol)	ln*A*	ΔH (kJ/mol)	ΔS (kJ/K)	ΔG (kJ/mol)
MPc1	412-520	0.020721	-5.58312	-6.22309	-160.512	120.53
MPc2	459-561	0.016762	-6.07138	-6.53467	-160.058	126.11
MPc3	460-584	0.011295	-7.01458	-6.63159	-161.544	129.06

Figure 5: XRD graphs of MPc1-3 complexes.

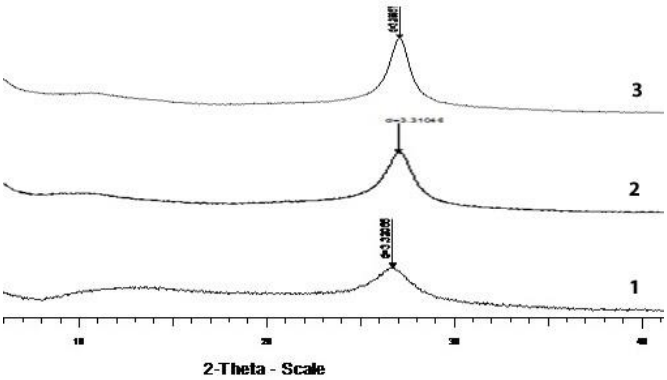

Figure 6: Variation of dielectric constant with frequency of MPc1-3 complexes.

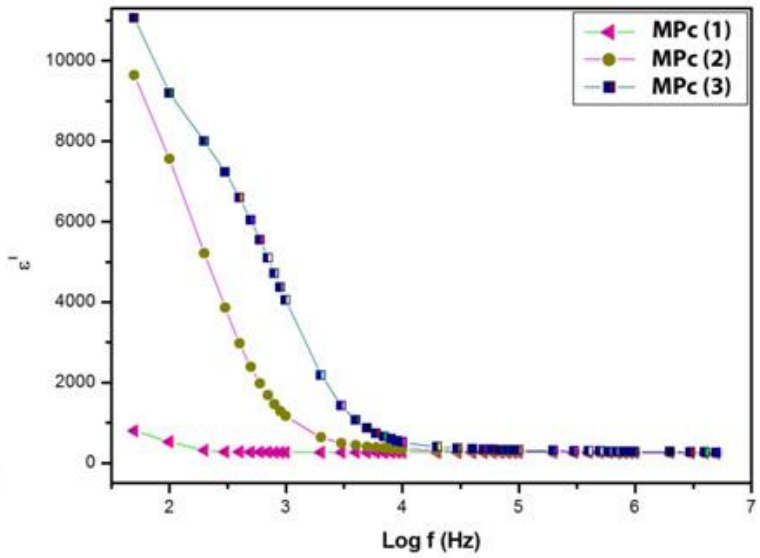

The Figure 7 shows the variation of dielectric loss tangent (tanδ) with frequency for the complexes MPc1-3 at room temperature. It is observed from the Figure 7 that the tanδ decreases with increasing frequency with shoulder nature for MPc2 and 3. The observation of shoulder in the MPc2 and 3 indicates the presence of resonance between the hopping frequency of the charge carriers and applied frequency. For MPc1 complex the shoulder behaviour is not observed in the measured frequency range. This is due to the resonance frequency for the MPc1 complex lie behind the frequency range of measurement [29]. All the resulting Pcs show low dielectric loss values in the measured frequency range and loss results supports to exploit these materials in the applications of high dielectric constant materials.

Figure 7: Variation of dielectric loss with frequency of MPc1-3 complexes.

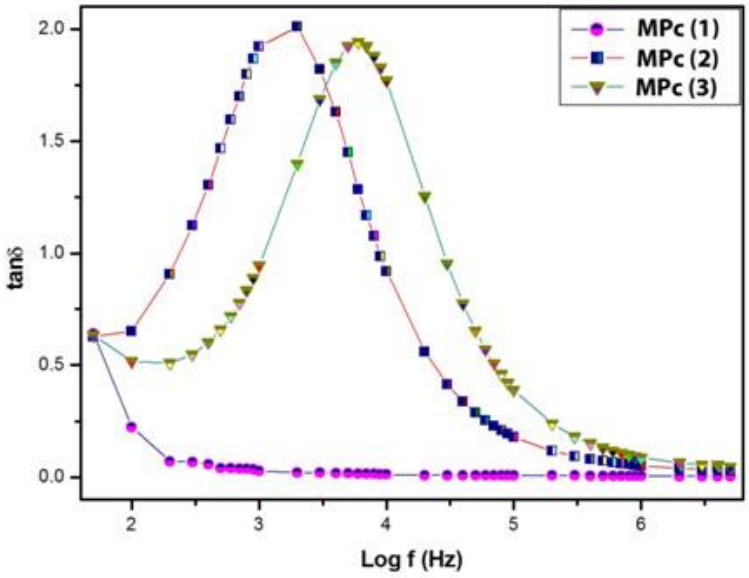

Figure 8 displays the frequency dependence of AC conductivity for MPc1-3 complexes at room temperature revealing an increasing trend in the conductivity with the increase of frequency, which is due to an increased density of charge carriers for conduction. In particular, the AC conductivity of the complex MPc1 is found to remain constant for increase in the frequency from 50 Hz to 1 MHz and found to increase suddenly for further increase in the frequency up to 5 MHz, whereas for the complexes MPc2 and 3, the AC conductivity is found to

increase with the increase in frequency from 50 Hz to 5 MHz. The observed trends in frequency dependence of AC conductivity can be explained on the basis of electron hopping model, that is, increase of conductivity with the increasing frequency [30] and the AC conductivity values are in the range of $4.0x10^{-5}$–$1.6x10^{-4}$ (S/m) at 5 MHz measured at 20 °C.

Figure 8: Variation of AC conductivity with frequency of MPc1-3 complexes.

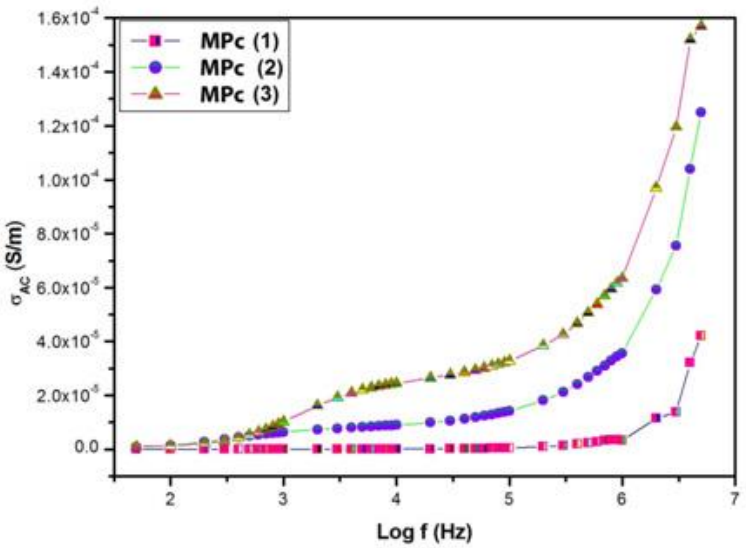

4. Conclusion

The metal phthalocyanine complexes embedded pyrido-[1,3,4]-oxadiazole moieties on peripheral position (MPc1-3) have been prepared and characterized. The ensuing complexes show admirable thermal stability (>400 °C) and exhibited maximum visible window absorption from 400 to 800 nm with decreased optical band gap. The AC conductivity for the MPc1-3 was explained by electron hopping model and the measured values are in the range of $4.0x10^{-5}$–$1.6x10^{-4}$ (S/m) at 5 MHz. However, in the MPc2 and MPc3, a shoulder nature is observed in the variation of tanδ with frequency, which is understood on the basis of resonance between hopping frequencies of charge carriers and applied frequency. The high dielectric constant (ε') (9800–11500 at 50 Hz) and low dielectric loss (tanδ) revealed by the MPc2 and 3 address its function in the field of sensors, actuators as well as bypass capacitors in microelectronics and energy-storage devices.

Competing Interests

The authors declare no conflict of interest.

Authors' Contributions

VKR was responsible for the project planning; PKM carried out the experiment, collected the data and wrote the manuscript; HMNK built the setup instruments. All authors discussed the results, read and approved the final manuscript.

Acknowledgement

The authors are grateful to the University Grants Commission, New Delhi, India, for their financial support and Indian Institute of Science, Bangalore, India, for providing solid-state ^{13}C-NMR spectra.

References

1. Amar NM, Saleh AM, Gould RD, 2003. Influence of temperature and frequency on the electrical parameters of thermally evaporated metal-free phthalocyanine H_2Pc thin films. Applied Physics A, 76: 77–82.
2. El-Nahass MM, Farid AM, Abd El-Rahman KF, Ali HAM, 2008. AC conductivity and dielectric properties of bulk tin phthalocyanine dichloride ($SnPcCl_2$). Physica B, 403: 2331–2337.
3. Abdel-Malik TG, Ahmed AA, Riad AS, 1990. Dark and photoelectric investigation on thin films of β-cobalt phthalocyanine dispersed in polymers. Physical Status Solidi A, 121: 507–513.

4. Henari FZ, 2001. Optical switching in organometallic phthalocyanine. Journal of Optics A: Pure and Applied Optics, 3: 188–190.
5. Chen Y, He N, Doyle JJ, Liu Y, Zhuang X, Blau WJ, 2007. Enhancement of optical limiting response by embedding gallium phthalocyanine into polymer host. Journal of Photochemistry and Photobiology, 189: 414–417.
6. Dini D, Barthel M, Hanack M, 2001. Phthalocyanines as active materials for optical limiting. European Journal of Organic Chemistry, 20: 3759–3769.
7. Guillaud G, Simon J, Germain JP, 1998. Metallophthalocyanines: Gas sensors, resistors and field effect transistors. Coordination Chemistry Reviews, 180: 1433–1484.
8. Panday RK, 2000. Recent advances in photodynamic therapy. Journal of Porphyrins and Phthalocyanines, 4: 368–373.
9. Xie D, Pan W, Jiang Yl, Li YR, 2007. Influence of α-alumina seed on the morphology of grain growth in alumina ceramics from Bayer aluminum hydroxide. Materials Letters, 57: 2395–2398.
10. Shankar R, Ghosh TK, Spontak R, 2007. Electroactive nanostructured polymers as tunable actuators. Advanced Materials, 19: 2218–2223.
11. Huang C, Zhang QM, de Botton G, Bhattacharya K, 2004. All-organic dielectric-percolative three-component composite materials with high electromechanical response. Applied Physics Letters, 84: 4391–4393.
12. Chiang CC, Chen H, Lee C, Leung M, Lin K, Hsieh K, 2008. Electrochemical deposition of Bis(*N,N'*-diphenylaminoaryl) substituted ferrocenes and their application as a hole-injection layer on polymeric light-emitting diodes. Chemistry of Materials, 20: 540–552.
13. Zhang P, Xia B, Zhang Q, Yang B, Li M, Zhang G, *et al.*, 2006. New 1,3,4-oxadiazole containing materials with the effective leading substituents: The electrochemical properties, optical absorptions, and the electronic structures. Synthetic Metals, 156: 705–713.
14. Klenkler RA, Aziz H, Tran A, Popovic ZD, Xu G, 2008. High electron mobility triazine for lower driving voltage and higher efficiency organic light emitting devices. Organic Electronics, 9: 285–290.
15. Chen S, Liu Y, Xu Y, Sun Y, Qiu W, Sun X, *et al.*, 2006. Langmuir–Blodgett film of new phthalocyanine containing oxadiazole groups and its application in field-effect transistor. Synthetic Metals, 156: 1236–1240.
16. Harish MNK, Keshavayya J, Reddy KRV, Mallikarjuna HR, Shoukat Ali RA, Rajesh T, 2010. Decorating nickel phthalocyanine periphery by aryl-1,3,4-oxadiazole pendants: Synthesis, characterization, and conductivity studies. Journal of Coordination Chemistry, 63: 4050–4060.
17. Harish MNK, Keshavayya J, Venugopala Reddy KR, Mallikarjuna HR, 2011. Designing nickel phthalocyanine periphery by alkyl chain via [1,3,4]-oxadiazole. Journal of Coordination Chemistry, 64: 2075–2087.
18. Maksimova KN, Bazyakina NL, Suvorova ON, Wöhrle D, 2011. Europium(iii) phthalocyanine complexes with 8-oxyquinoline. Russian Chemical Bulletin, International Edition, 60: 269–272.
19. Bıyıklıoglu Z, Kantekin H, 2011. Synthesis and spectroscopic properties of a series of octacationic water-soluble phthalocyanines. Synthetic Metals, 161: 943–948.
20. Erdogmus A, Nyokong T, 2010. Synthesis of zinc phthalocyanine derivatives with improved photophysicochemical properties in aqueous media. Journal of Molecular Structure, 977: 26–38.
21. Sharma AK, Bhatia KL, 1989. Frequency-dependent electrical conductivity of bismuth-modified amorphous semiconductors $(GeSe_{3.5})_{100-x}Bi_x$. Journal of Non-Crystalline Solids, 109: 95–104.
22. Song X, She Y, Ji H, Zhang Y, 2005. Highly efficient, mild, bromide-free and acetic acid-free dioxygen oxidation of *p*-Nitrotoluene to *p*-Nitrobenzoic acid with metal phthalocyanine catalysts. Organic Process Research and Development, 9: 297–301.
23. Maya EM, de la Torre G, Lozano AE, Torres T, de la Campa JG, de Abajo J, 2006. Novel cobalt (II) phthalocyanine-containing polyimides: Synthesis, characterization, thermal and optical properties. Macromolecular Rapid Communications, 27: 1852–1858.
24. Ahsen V, Yilmazer E, Ertas M, Bekaroglu O, 1988. Synthesis and characterization of metal-free and metal derivatives of a novel soluble crown-ether-containing phthalocyanine. Journal of the Chemical Society, Dalton Transactions, 40: 401–406.
25. Liu Y, Lin H, Li X, Li J, Nan H, 2010. Photoinduced electron transfer in panchromatic zinc phthalocyanine–azobenzene dyad. Inorganic Chemistry Communications, 13: 187–190.
26. Broido AA, 1969. Simple, sensitive graphical method of treating thermogravimetric analysis data. Journal of Polymer Science Part B: Polymer Physics, 7: 1761–1773.
27. Ray AK, Tracey SM, Hassan AK, 1996. Conduction in partially monoclinic films of lead phthalocyanine. IEE Proceedings of Science, Measurement and Technology, 146: 205–209.
28. Sidebottom DL, Rolling B, Funke K, 2000. Comparing conductivity and modulus representations with regard to scaling properties and ionic conduction in solids. Physical Review B: Condensed Matter, 63: 24301/1–24301/7.
29. Sheikh AD, Mathe VL, 2008. Anomalous electrical properties of nanocrystalline Ni–Zn ferrite. Journal of Materials Science, 43: 2018–2025.
30. Anthopoulos TD, Shafai TS, 2003. Alternating current conduction properties of thermally evaporated α-nickel phthalocyanine thin films: Effects of oxygen doping and thermal annealing. Journal of Applied Physics, 94: 2426–2433.

How to cite this article:

Musturappa PK *et al.*, 2013. New Metallophthalocyanines Posture Pyridine Pendants Via 1,3,4-Oxadiazole Bridge: Synthesis, Optical and Electrical Studies. Chemical Sciences Journal, Vol. 2013: 10 pages, Article ID: CSJ-105.